The American Journal of Sports Medicine

http://ajs.sagepub.com/

The Distal Triceps Tendon Footprint and a Biomechanical Analysis of 3 Repair Techniques

Peter C. Yeh, Kelly T. Stephens, Olga Solovyova, Elifho Obopilwe, Lawson R. Smart, Augustus D. Mazzocca and Paul M. Sethi

Am J Sports Med 2010 38: 1025 originally published online March 3, 2010
DOI: 10.1177/0363546509358319

The online version of this article can be found at:
http://ajs.sagepub.com/content/38/5/1025

Published by:
SAGE
http://www.sagepublications.com

On behalf of:
AOSSM
American Orthopaedic Society for Sports Medicine

The Distal Triceps Tendon Footprint and a Biomechanical Analysis of 3 Repair Techniques

Peter C. Yeh,*† MD, Kelly T. Stephens,‡ ME, Olga Solovyova,‡ Elifho Obopilwe,‡ ME, Lawson R. Smart,§ MD, Augustus D. Mazzocca,‡ MD, and Paul M. Sethi,†‖ MD

From the †Department of Orthopaedics and Rehabilitation, Yale University School of Medicine, New Haven, Connecticut, ‡Human Soft Tissue Research Laboratory, New England Musculoskeletal Institute, University of Connecticut Health Center, Farmington, Connecticut, §New England Baptist Hospital, Boston, Massachusetts, and the ‖ONS Foundation for Clinical Research and Education, Greenwich, Connecticut

Background: Anatomic repair of tendon ruptures is an important goal of surgical treatment. There are limited data on the triceps brachii insertion, footprint, and anatomic reconstruction of the distal triceps tendon.

Hypothesis: An anatomic repair of distal triceps tendon ruptures more closely imitates the preinjury anatomy and may result in a more durable repair.

Study Design: Descriptive and controlled laboratory studies.

Methods: The triceps tendon footprint was measured in 27 cadaveric elbows, and a distal tendon rupture was created. Elbows were randomly assigned to 1 of 3 repair groups: cruciate repair group, suture anchor group, and anatomic repair group. Biomechanical measurement of load at yield and peak load were measured. Cyclic loading was performed for a total of 1500 cycles and displacement measured.

Results: The average bony footprint of the triceps tendon was 466 mm^2. Cyclic loading of tendons from the 3 repair types demonstrated that the anatomic repair produced the least amount of displacement when compared with the other repair types ($P <$ .05). Load at yield and peak load were similar for all repair types ($P >$ .05).

Conclusion: The triceps bony footprint is a large area on the olecranon that should be considered when repairing distal triceps tendon ruptures. Anatomic repair of triceps tendon ruptures demonstrated the most anatomic restoration of distal triceps ruptures and showed statistically significantly less repair-site motion when cyclically loaded.

Clinical Relevance: Anatomic repair better restores preinjury anatomy compared with other types of repairs and demonstrates less repair-site motion, which may play a role in early postoperative management.

Keywords: triceps; tendon ruptures; suture bridge; footprint; olecranon

Distal rupture of the triceps tendon is a rare injury and is among the least common of reported tendon injuries. In a review of 1014 tendon ruptures, 0.8% constituted triceps tendon injuries.[1] Over a 10-year span, only 12 cases of triceps rupture were recorded in the National Football League.[6] There is a male predominance of roughly 2 to 1 throughout all ages.

The most common mechanism of injury is a sudden eccentric load applied to a contracting triceps muscle such as a fall onto an outstretched hand or during weight lifting. Regardless of mechanism, ruptures are usually seen at the osseous insertion.[13,15] However, rupture within the muscle belly has been reported,[8] as well as tears at the myotendinous junction.[3,16] By far, the most common primary repair technique involves the transosseous cruciate repair technique for distal ruptures described by van Riet et al.[15] In their study, a 21% rerupture rate was reported.

The tendon footprint of the rotator cuff and biceps insertion has been studied,[2,7,10,11] and anatomic repair techniques have been described.[9] Despite the ubiquity of the triceps-splitting, triceps-sparing, and triceps-reflecting

*Address correspondence to Peter C. Yeh, MD, Yale Physicians Building, 800 Howard Avenue, 133YPB, New Haven, CT 06519 (e-mail: pda@aya.yale.edu).

Presented at the 35th annual meeting of the AOSSM, Keystone, Colorado, July 2009.

One or more of the authors has declared a potential conflict of interest: all suture anchors in this study were provided by Arthrex.

The American Journal of Sports Medicine, Vol. 38, No. 5
DOI: 10.1177/0363546509358319

approaches to the distal humerus and proximal forearm, the distal triceps tendon insertion site on the olecranon has not been studied extensively. This is likely because triceps tendon injuries such as ruptures are a rare entity.[1,6] Nevertheless, the insertion area of the triceps tendon is particularly important to understand when considering triceps tendon repair. Extension strength of the elbow is associated with the insertion-site integrity of the triceps.[19] We hypothesize that there is a relationship between the amount of footprint restored in a tendon repair and its resultant strength and resistance to gap formation.

Surgical repair is generally performed for active individuals with complete triceps tendon ruptures or incomplete ruptures with loss of strength. A thorough understanding of the insertion-site anatomy is paramount when treating distal triceps tendon ruptures.

These injuries have been traditionally repaired with a transosseous cruciate suture technique. This technique involves the reattachment of the ruptured tendon to a point onto the olecranon. The results of this surgical repair are subjectively reported to be good to excellent. However, objective evidence is limited and has only been seen in case reports and series. Furthermore, reruptures of previously repaired triceps ruptures are well described.[6,12-15,18] The purpose of this study is twofold: first, to examine and fully describe the anatomy of the triceps tendon insertion and second, to objectively compare an anatomic repair technique with a cruciate repair as well as a suture anchor repair for triceps tendon ruptures.

METHODS

Twenty-seven cadaveric elbows were obtained and used in this study. The anatomic portion of the study was performed first. The elbow was dissected to expose the tendinous insertion of the triceps onto the olecranon. The triceps tendon was then dissected off its bony insertion. Several measurements were made with a gliding digital caliper. The length and width of the triceps tendon at the insertion, the distance from the tip of the olecranon to the articular surface, and the width of the lateral triceps expansion were measured and the area of the triceps bony insertion "footprint" was then calculated using the formula area = length × width. Each variable was measured 3 times with the gliding digital caliper, which allows measuring distances down to 0.01 mm. These values were then averaged.

Three treatment groups were then devised and each elbow was randomly assigned to a treatment group: transosseous cruciate repair, suture anchor repair, and anatomic repair. The triceps was then repaired per the predetermined repair method.

Transosseous Cruciate Repair Technique

This repair was performed via the description of the transosseous cruciate repair technique of van Riet et al.[15] The tendon ends are minimally debrided such that fresh tendinous tissue is exposed. A Krackow-type whipstitch with a #2 nonabsorbable FiberWire suture (Arthrex, Naples, Florida) is first passed through the end of the ruptured tendon. Four passes of the whipstitch are made on each side of the tendon with the same suture. Two crossing transosseous drill holes are made on the olecranon parallel to the joint surface. These crossing drill holes were made by best approximating the center of the footprint and ensuring that the holes were made 11.75 mm distal to the tip of the olecranon (to avoid joint penetration). Each strand of the suture is passed into each drill hole from proximal to distal and tied (with 5 alternating half-hitch knots) to each other over the bone bridge (Figure 1).

Suture Anchor Repair Technique

Two metal 4.5-mm suture anchors (Arthrex) are placed in the middle of the footprint, with use of the dead man's angle, aimed away from the joint. A #2 nonabsorbable FiberWire suture is passed in a Krackow-type whipstitch fashion. Four passes of the whipstitch are made on each side of the tendon with the same suture. Each strand from the whipstitch is tied down to each suture anchor with 5 alternating half-hitch knots each (Figure 2).

Anatomic Repair Technique

A transosseous-equivalent footprint repair of the triceps is performed similar to that recently described in the rotator cuff.[9] The bony insertion site is excoriated to remove any interposed soft tissue. A locking-type whipstitch (ie, Krackow) is placed through the tendon utilizing 4 throws on each side of the tendon with both ends of the suture free at the edge of the proximal tendon.

Two 3.0-mm press-fit bioabsorbable anchors (BioSuture Tak, Arthrex) are placed on the proximal end of the footprint site, 1 on the lateral edge and the other on the medial edge. Based on this anatomic study, the distance from the tip of the olecranon to the articular surface is 11.75 mm. As such, the anchors are placed 13 mm distal to the tip of the olecranon and directed distal to the articular surface to avoid the risk of joint penetration, while at the same time keeping as close as possible to the dead man's angle. It should be made clear that these anchors are placed on the proximal end of the footprint, similar to the medial row of anchors in a rotator cuff repair. Another row of anchors is subsequently placed distal to the footprint, allowing maximal surface area coverage of the repaired tendon to the footprint.

A mattress suture from each anchor is placed in the distal tendon 2 cm proximal to the end. This secures the proximal tendon down to the bone and restores the distinct medial (medial-sided anchor) and lateral (lateral-sided anchor) insertion. The sutures should not be cut.

The distal footprint is estimated (the tendon distal to the secured anchors is laid down on the olecranon) and 2 pilot holes are created to accommodate the next 2 anchors. The holes should be placed just distal to the anatomic footprint and care should be taken not to drill directly toward the joint surface, but obliquely, aiming distally on the ulnar shaft while also conforming to the dead man's angle.

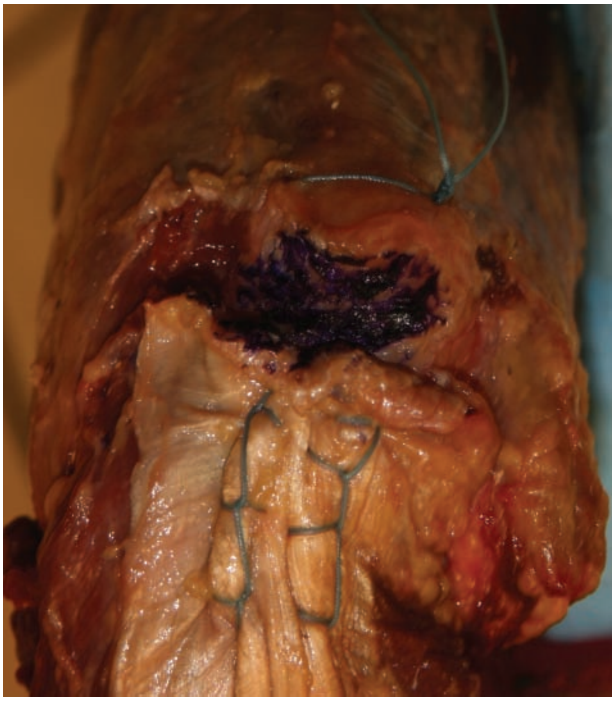

Figure 1. The transosseous cruciate repair. The suture ends on the ulna are tied down over a bone bridge with the purple markers indicating the triceps footprint that is still exposed (pre–cyclic loaded). At least 8 to 10 mm of the footprint is still exposed distally. Reflection of the tendon also yields the uncovered footprint proximally.

Figure 2. The suture anchor repair. A smaller region of footprint (6-8 mm) is exposed.

One tail from each anchor and 1 limb of the free Krackow (total of 3 sutures) are then threaded into the anchor eyelet of a 3.5-mm PushLock anchor (Arthrex). With tension being held on the sutures (reducing the

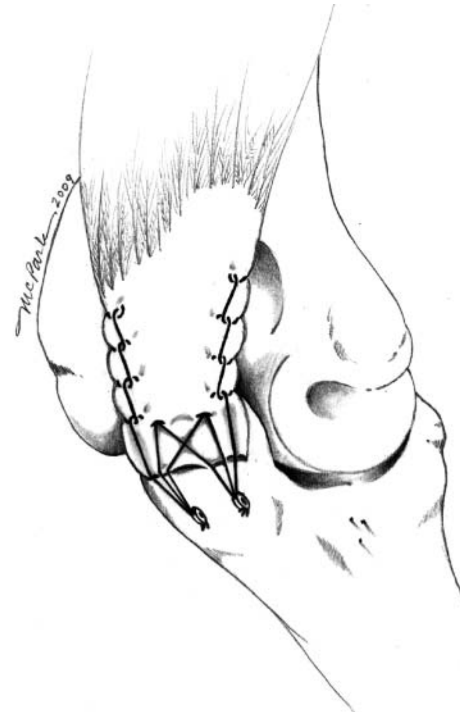

Figure 3. Triceps tendon repair using an anatomic repair technique. Reproduced with permission Maxwell C. Park, MD.

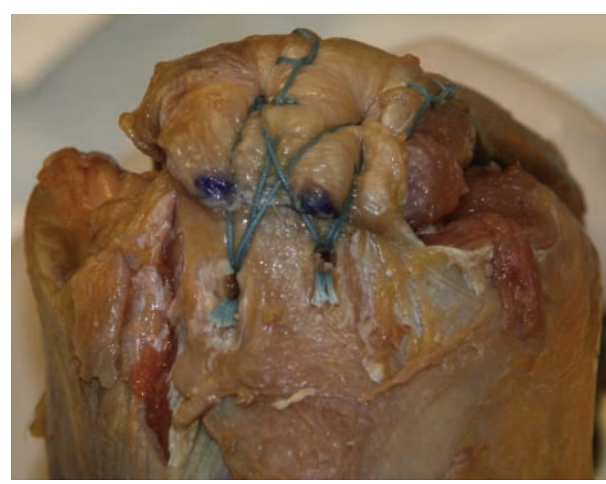

Figure 4. Anatomic repair. Near-complete coverage of the triceps footprint is achieved with no purple markings exposed (pre–cyclic loaded).

tendon to its desired position on the footprint), the anchor is advanced with a mallet into the pilot hole until flush. To avoid differences, 1 surgeon (P.M.S.) was used to gauge tension. The sutures can then be cut flush. The remaining sutures are threaded into the eyelet of a second PushLock anchor and this is driven into the other pilot hole with the suture ends cut flush (Figures 3 and 4).

Biomechanical Testing

The proximal end of the humerus was potted in orthodontic bone cement for fixture attachment and reinforced with threaded screws. The elbow was fixed at the proximal end of the humerus using the MTS custom fixture (MTS Systems, Eden Prairie, Minnesota). Upon testing, a 2-lb free weight was placed 8 inches from the tip of the olecranon to minimize momentum. The triceps tendon was attached to a 2500-N load cell by a polypropylene connecting strap and a pulley (Figure 5A).

The 2-lb weight was determined based on the finding of a pilot study during which a frequency of 1 Hz was used during cyclic loading; however, this speed and momentum produced a violent cyclic pattern of motion in the triceps, causing the belly of the triceps muscle to tear from the loading strap. Instead, a 0.25-Hz frequency was used with the weight placed 8 inches from the olecranon based on the anthropometric measurements and findings of Webb Associates[17] for body-segment link length values and percentage distribution of total body weight according to different segmentation plans.

For both intact and repaired states, the triceps tendon was preconditioned from 0° to 90° for 10 cycles at a rate of 0.25 Hz. The triceps tendon was tested from 0° to 90° for 1500 cycles at a rate of 0.25Hz. Two differential variable reluctance transducers (Microstrain, Burlington, Vermont) were placed 1 cm apart on the tendon for the purpose of measuring displacement of the tendon during cyclic loading (Figure 5B). Load-to-failure was performed at a rate of 120 mm/min. Displacements were recorded, and repaired displacement values were compared with the same intact elbow displacement. Failure of the construct was considered when there was greater than 10 mm of displacement of the tendon from the bone tunnel. Footprint restoration assessment was made for each repair with the MicroScribe G2 3D Digitizer (Immersion, San Jose, California) and Rhinoceros modeling software (Robert McNeel & Associates, Seattle, Washington).

Statistical Method

All standard deviations were calculated in standard fashion and statistical comparisons were performed using SPSS 17.0 (SPSS Inc, Chicago, Illinois). A 1-way analysis of variance with Bonferroni post hoc pairwise comparison was used to identify differences in mean displacement between the 4 study groups (intact elbow, anatomic, cruciate repair, and suture anchor). Statistical significance was established at a 2-sided alpha level of .05 ($P < .05$).

RESULTS

Anatomic Study

The average age of the cadaveric elbows was 61 ± 11 years. The average triceps width in its entirety (including both tendon and lateral expansion) at the insertion was 40.60 mm (standard deviation [SD] ± 5.97). The average triceps

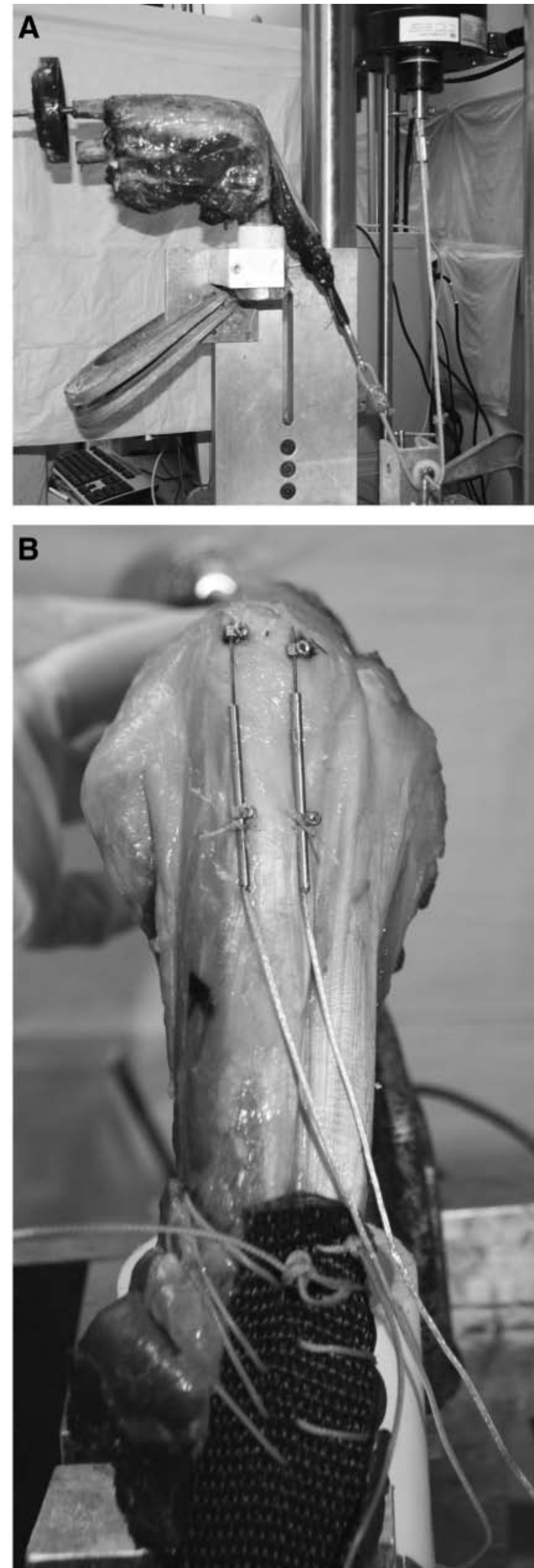

Figure 5. A, biomechanical testing setup. B, transducer setup; 2 differential variable reluctance transducers were placed 1 cm apart on the tendon to measure displacement.

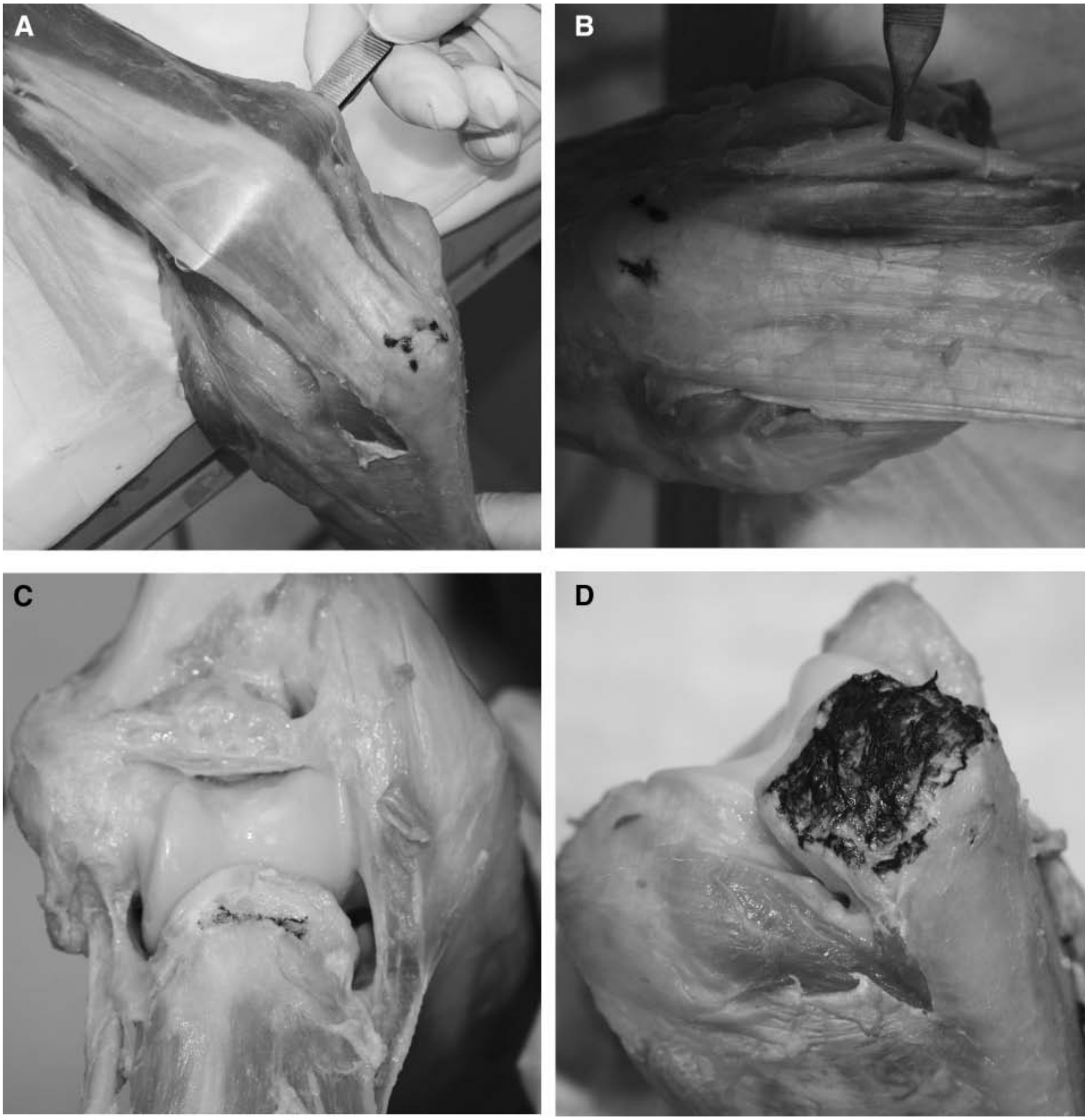

Figure 6. A, complete triceps tendon (including tendon proper and lateral expansion). B, ulnar nerve (being grasped by forceps) to tendon distance. C, proximal insertion of the triceps. The native triceps tendon is reflected and the joint capsule removed. The tip of the olecranon is visible. The line demarcates the insertion of the distal triceps. This was routinely proximal to the articular surface of the olecranon. D, the native triceps footprint is outlined in marker, demonstrating the wide footprint.

tendon width was 30.56 mm (SD ± 7.17). The average lateral expansion width was 14.36 mm (SD ± 3.73) (Figure 6A). The average distance from the medial edge of the tendon to the ulnar nerve was 10.20 mm (SD ± 4.11) (Figure 6B). The average distance from the olecranon tip to the level of the articular surface was 11.75 mm (SD ± 3.16) (Figure 6C). The average bony footprint length and width were 20.52 mm (SD ± 2.02) and 22.65 mm (SD ± 2.40), respectively (Figure 6D). The average triceps bony insertion footprint area was found to be 466.16 mm^2 (SD ± 78.63) (Table 1).

Qualitative assessment of the 3 repairs revealed 3 distinct patterns of footprint coverage. The transosseous cruciate repair yielded point fixation on the olecranon, with at least 8 to 10 mm of footprint length exposed proximally and distally. This translates to the repair covering an average of 146 mm^2 (31%) of the footprint (Figure 1). The suture anchor repair yielded a repair that had both proximal

TABLE 1
Averaged Anatomic Measurements of All Elbows

	Olecranon Width, mm	Tendon Width, mm	Tendon Only, mm	Tendon to Ulnar Nerve, mm	Lateral Expansion, mm	Footprint Bone Length, mm	Footprint Bone Width, mm	Footprint Area, mm^2	Olecranon Tip to Articular Surface, mm
Average	25.38	40.60	30.56	10.20	14.36	20.52	22.65	466.16	11.75
Standard deviation	3.84	5.97	7.17	4.11	3.73	2.02	2.40	78.63	3.16

and distal footprint exposed, but to a lesser degree than the transosseous cruciate repair, with 6 to 8 mm total left on both sides combined; thus an average of 226 mm^2 (48%) of the footprint was covered (Figure 2). The anatomic repair restored all but the native proximal insertion with 1 to 2 mm exposed proximally and no footprint exposure distally, thus covering 400 mm^2 (86%) of the footprint (Figure 7).

Biomechanical Study

An a priori power analysis was performed with regard to the load variables that showed, for an effect size of 50% and an alpha of .05, 26 cases would provide a study power of 0.80.

Each cadaveric tendon repair, as well as unrepaired, intact tendons, which acted as controls, underwent cyclic loading. After 1500 cycles, the average displacement of the intact tendon was 0.31 mm (SD ± 0.28) on the medial side and 0.32 mm (SD ± 0.25) on the lateral side of the tendon. The average displacement of the transosseous cruciate repair was 3.21 mm (SD ± 2.00) on the medial side and 2.99 mm (SD ± 1.76) on the lateral side. The average displacement of the tendon in the anatomic repair was 1.16 mm on both the medial (SD ± 0.73) and lateral (SD ± 0.82) sides. The average displacement of the suture anchor repair was 1.96 mm (SD ± 0.52) on the medial side and 1.93 mm (SD ± 0.64) on the lateral side (Table 2 and Figure 8). Among the repaired tendons, the average displacement was the greatest for the transosseous cruciate repair and the least with the anatomic repair ($P < .05$) (Table 3).

The appearance of the tendon repair after cyclic loading differed considerably between the 3 repairs. The tendon repair was pulled away from the footprint area in both the suture anchor and cruciate repairs, and the integrity of the tendon was uniformly injured with intratendinous rupture and fraying (Figures 9 and 10). However, in the anatomic repair, the appearance was essentially unchanged from the beginning to the end of the 1500 cycles (Figure 11).

One failure (ie, breakage of suture or rerupture of tendon) occurred during the 1500-cycle loading. The failure was in the suture anchor group. Footprint coverage was examined after cyclic loading, but could not be quantified in an accurate fashion and therefore is not presented here. This is because after cyclic loading, the laxity of the sutures in the suture anchor and cruciate repairs when the tendon was reflected allowed for an overestimation of the proximal footprint that was uncovered. Combining this with the laxity of the sutures when measuring the distal footprint that was uncovered with the tendon not reflected, one theoretically may calculate a value larger than the total footprint area.

Mechanisms of failure occurred in several manners. In the cruciate repair group, 6 failures occurred at the suture-tendon interface, causing a tear through the tendon. In another, a tear at the tendon was seen along with the failure occurring as a break in the suture within the tendon. In 2, the suture pulled through the tendon without breakage or loosening.

In the suture anchor repair group, failure of the repair occurred with suture breakage within the anchor in all but 1. This repair failed with lateral suture breakage followed by medial anchor pullout. However, this was the only failure with an anchor-pullout failure mode.

In the anatomic repair group, failure was from breakage of suture within an anchor. In all but 1 of the repairs, breakage occurred in the medial anchor first; in another, simultaneous breakage of sutures from both anchors occurred. Pullout of the anchors occurred in only 1 repair in this group.

Load at yield and peak load for the various repairs are shown in Table 4. The anatomic repair group had the highest load at yield and peak load; however, this was not statistically significant.

DISCUSSION

We describe the native triceps tendon footprint and the biomechanical properties of 3 distal triceps tendon repair techniques. The anatomic repair technique is a tendon repair technique that mirrors surgical repair studied in rotator cuff repairs. The basis is predicated on recreating the preinjury anatomy with uniform distribution of pressure on the repair. Although the clinical relevance is still unclear, restoration of the anatomy appears to be a useful surgical principle.

The triceps footprint covers a large area of the olecranon, averaging 466 mm^2 in this study. In fact, the tendon width at the insertion was found to be greater than the olecranon width, indicating that the distal triceps does not end at a point insertion, but one that extends well distal to the olecranon tip and includes the medial and lateral borders of the olecranon. The triceps possesses a large area

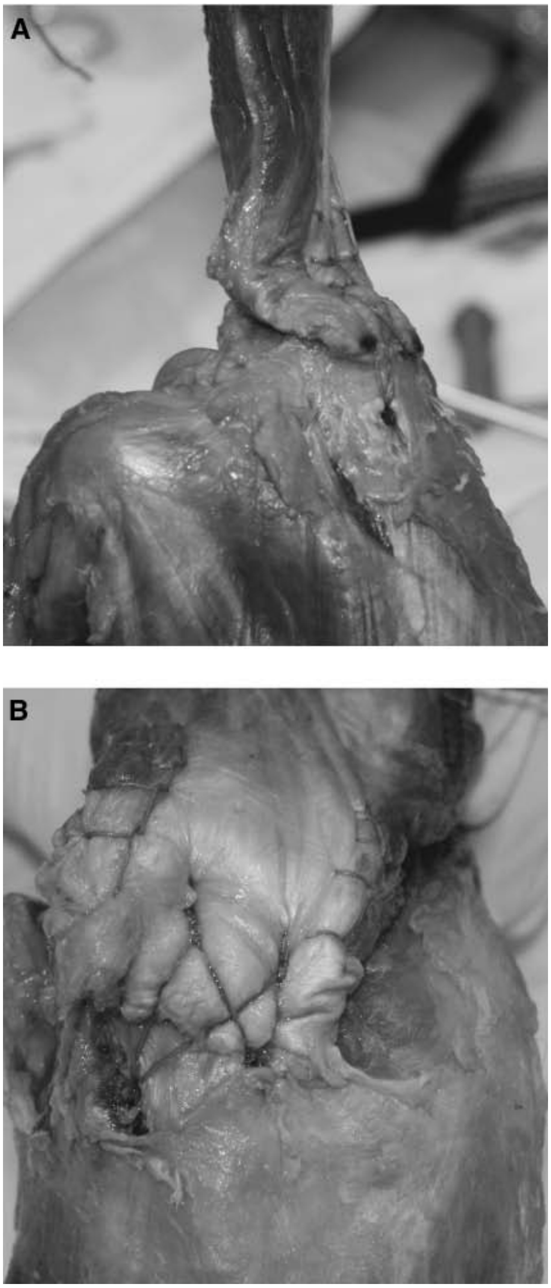

Figure 7. Anatomic repair. A, lateral view demonstrates near-complete coverage of the distal and proximal ends. B, AP view demonstrates near-complete coverage of the footprint.

TABLE 2
Amount of Displacement After 1500 Cycles, in Millimeters[a]

	Intact		Cruciate		Anatomic		Suture Anchor	
	Mean	SD	Mean	SD	Mean	SD	Mean	SD
Medial epicondyle	0.31	.028	3.21	2.00	1.16	0.73	1.96	0.52
Lateral epicondyle	0.32	0.25	2.99	1.76	1.16	0.82	1.93	0.64

[a]Averaged values of the 3 repair techniques along with intact tendon after cyclic loading. All values were significant ($P < .05$). SD, standard deviation.

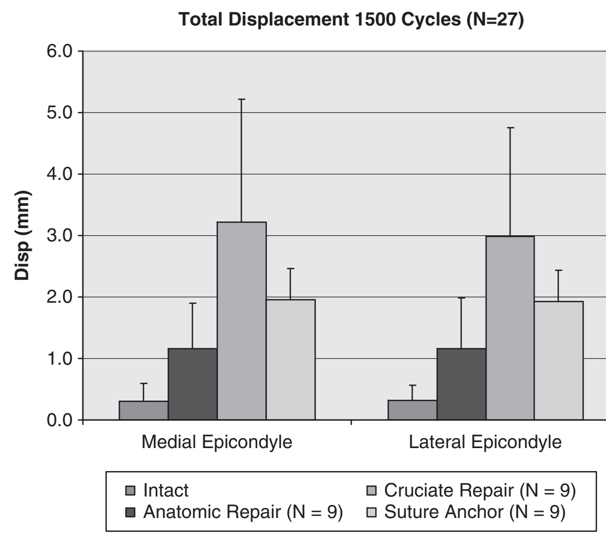

Figure 8. Average total displacement. After 1500 cycles of loading, displacement was measured for intact tendons as well as the 3 repair techniques. The anatomic repair yielded the least amount of displacement and very closely mimicked intact tendon cyclic-loading properties ($P < .05$).

of contact at the insertion as it is the dominant structure of the posterior humerus, allowing many activities including activities of daily living (eg, getting up from a chair). The lateral expansion of the triceps was roughly half the average width of the tendon itself at the bony insertion (14.36 mm and 30.56 mm, respectively). This is a large percentage contribution to the complete tendinous insertion and underscores the importance of repairing the lateral expansion for triceps tendon ruptures, perhaps similar to repairing the medial retinaculum in quadriceps tendon ruptures, and may explain the presence of active elbow extension in the setting of a full-thickness tendon rupture. The distance between the medial border of the tendon at the insertion to the ulnar nerve is on average 10.2 mm. This highlights the proximity of the neurovascular structures in this soft tissue repair.

Of the 3 repairs, the anatomic repair most accurately restored the anatomic footprint, covering 86% of the footprint. The other 2 repair techniques left large areas of the footprint uncovered, with 48% footprint coverage with suture anchors and 31% coverage with the transosseous cruciate technique. The anatomic repair did not cover the most proximal aspect of the triceps footprint because placing suture anchors at this point would risk penetration into the articular surface.

The differences in footprint restoration were even more pronounced after cyclic loading (Figures 9-11), with essentially no change in the anatomic repair group and

TABLE 3
P Values for Displacement After 1500 Cycles[a]

	Family *P* value	Intact vs Anatomic	Intact vs Cruciate	Intact vs Suture Anchor	Anatomic vs Cruciate	Anatomic vs Suture Anchor	Cruciate vs Suture Anchor
Medial epicondyle	<.001	.152	<.001	.003	<.001	.4	.082
Lateral epicondyle	<.001	.094	<.001	.001	.001	.35	.121

[a]Analysis of variance power analysis for overall (family) and individual comparisons.

TABLE 4
Average Failure Load Results[a]

Repair Type	Load at Yield, N	SD	Peak Load, N	SD
Anatomic	465.87	121.03	592.44	75.49
Suture anchor	340.21	185.48	508.57	320.92
Cruciate	370.25	277.65	579.62	232.11
P values				
Anatomic vs Cruciate	Suture Anchor vs Cruciate	Suture Anchor vs Anatomic		
.44	.33	.24		

[a]Although the anatomic repair yielded the highest load at yield and highest peak load, this was not significant ($P > .05$). SD, standard deviation.

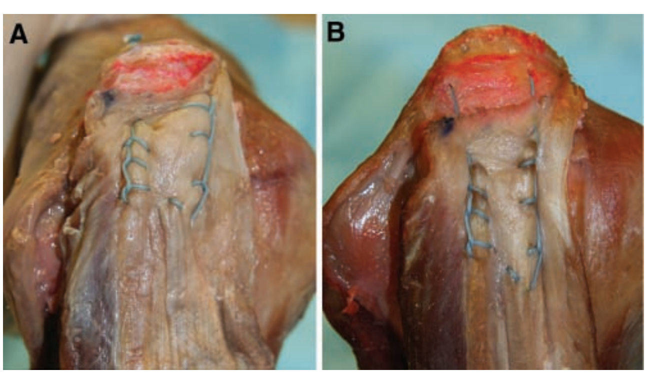

Figure 9. Cruciate repair before (A) and after (B) cyclic loading; 69% of the footprint is uncovered before cyclic loading and even more evident after the 1500 cycles.

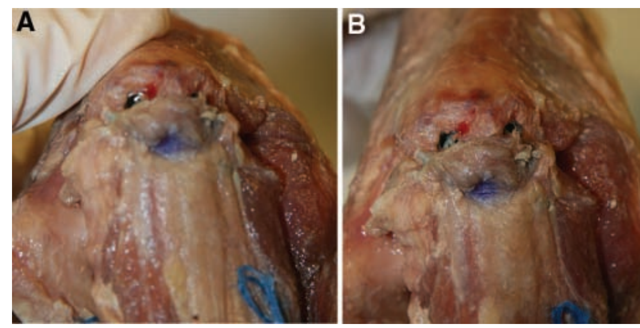

Figure 10. Suture anchor repair before (A) and after (B) cyclic loading; 52% of the footprint is uncovered before 1500 cycles of loading and more pronounced after loading.

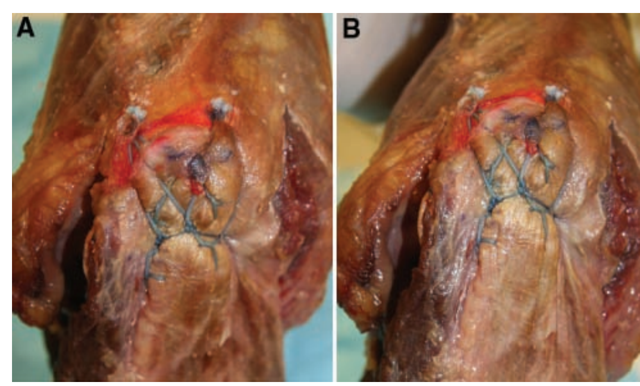

Figure 11. Anatomic repair before (A) and after (B) cyclic loading; 14% of the footprint has been uncovered after 1500 cycles of loading.

pronounced gapping in the cruciate repair group. Although these are not quantitative data, the appearance of the cycled repairs is compelling and warrants attention. What significance this has on healing cannot be answered objectively within the scope of this study.

Displacement after cyclic loading was highest in the transosseous cruciate repair and lowest in the anatomic repair. This was statistically significant ($P < .05$) and suggests that with the cruciate repair, significant gap formation is seen when compared with the anatomic repair. There is evidence in the literature to suggest that gap formation in rotator cuff repairs has been associated with poor healing[4,5] and may suggest that clinically, postoperative range of motion restrictions need to be maintained for the cruciate repairs. The suture anchor group was the only subset to have a failure during cyclic loading.

The peak load and load at yield was similar for all 3 constructs and was seen to fail at the suture or suture-anchor interface. This suggests that the mode of failure was more related to the mechanical properties of the suture material rather than the type of repair. Furthermore, the materials of the implants had little effect on the biomechanical repair characteristics studied here. This is demonstrated by the use of metal anchors in the suture anchor group whereas in the anatomic repair group, polyetheretherketone (PEEK) anchors were used.

To date, our clinical results with the use of this technique have been very satisfying. We have had no failures and have had excellent subjective outcomes with 6 repairs, including 1 revision. Long-term follow-up and objective grading of this small subset is underway.

One limitation of this study was the lack of an objective measure to study pressure and contact area characteristics of the various repairs before and after cyclic loading. We attempted to digitally measure and quantify the postloading footprint but found this to be unreliable (secondary to the laxity of the sutures after cycling) and dependent on the position of the tendon (ie, held anatomically in place versus reflected back); as such, quantitative data on footprint coverage after loading are not reported. The use of a tactile pressure measurement such as a TekScan I-Scan Pressure Measurement System (TekScan, South Boston, Massachusetts) or pressure-sensitive film would certainly be a valid follow-up investigation. Another drawback to this study is the use of cadaveric specimens. The cyclic loading was performed on nonhealing tissue, immediately after repair of a cadaveric elbow. Lastly, because this was a biomechanical, cadaveric study, long-term functional results of these repairs cannot be gleaned, but certainly would be a valid area of investigation for future studies.

The triceps bony footprint is a large area measuring on average 466 mm^2. Anatomic repair of acute triceps tendon ruptures demonstrated the most anatomic restoration of distal triceps ruptures and possessed the least amount of repair-site motion when cyclically loaded.

ACKNOWLEDGMENT

The authors thank Maxwell C. Park, MD, for his illustration.

REFERENCES

1. Anzel SH, Covey KW, Weiner AD, Lipscomb PR. Disruption of muscles and tendons: an analysis of 1,014 cases. *Surgery*. 1959;45(3):406-414.
2. Athwal GS, Steinmann SP, Rispoli DM. The distal biceps tendon: footprint and relevant clinical anatomy. *J Hand Surg Am*. 2007;32(8):1225-1229.
3. Bach BR Jr, Warren RF, Wickiewicz TL. Triceps rupture: a case report and literature review. *Am J Sports Med*. 1987;15(3):285-289.
4. Burkhart SS, Diaz Pagan JL, Wirth MA, Athanasiou KA. Cyclic loading of anchor-based rotator cuff repairs: confirmation of the tension overload phenomenon and comparison of suture anchor fixation with transosseous fixation. *Arthroscopy*. 1997;13(6):720-724.
5. Gerber C, Schneeberger AG, Beck M, Schlegel U. Mechanical strength of repairs of the rotator cuff. *J Bone Joint Surg Br*. 1994;76(3):371-380.
6. Mair SD, Isbell WM, Gill TJ, Schlegel TF, Hawkins RJ. Triceps tendon ruptures in professional football players. *Am J Sports Med*. 2004;32(2):431-434.
7. Mazzocca AD, Cohen M, Berkson E, et al. The anatomy of the bicipital tuberosity and distal biceps tendon. *J Shoulder Elbow Surg*. 2007;16(1):122-127.
8. O'Driscoll SW. Intramuscular triceps rupture. *Can J Surg*. 1992;35(2): 203-207.
9. Park MC, Elattrache NS, Ahmad CS, Tibone JE. ''Transosseous-equivalent'' rotator cuff repair technique. *Arthroscopy*. 2006;22(12): 1360.
10. Park MC, ElAttrache NS, Tibone JE, Ahmad CS, Jun BJ, Lee TQ. Part I: footprint contact characteristics for a transosseous-equivalent rotator cuff repair technique compared with a double-row repair technique. *J Shoulder Elbow Surg*. 2007;16(4):461-468.
11. Park MC, Tibone JE, ElAttrache NS, Ahmad CS, Jun BJ, Lee TQ. Part II: biomechanical assessment for a footprint-restoring transosseous-equivalent rotator cuff repair technique compared with a double-row repair technique. *J Shoulder Elbow Surg*. 2007;16(4):469-476.
12. Sierra RJ, Weiss NG, Shrader MW, Steinmann SP. Acute triceps ruptures: case report and retrospective chart review. *J Shoulder Elbow Surg*. 2006;15(1):130-134.
13. Sollender JL, Rayan GM, Barden GA. Triceps tendon rupture in weight lifters. *J Shoulder Elbow Surg*. 1998;7(2):151-153.
14. Strauch RJ. Biceps and triceps injuries of the elbow. *Orthop Clin North Am*. 1999;30(1):95-107.
15. van Riet RP, Morrey BF, Ho E, O'Driscoll SW. Surgical treatment of distal triceps ruptures. *J Bone Joint Surg Am*. 2003;85(10):1961-1967.
16. Wagner JR, Cooney WP. Rupture of the triceps muscle at the musculotendinous junction: a case report. *J Hand Surg Am*. 1997; 22(2):341-343.
17. Webb Associates. *Anthropometric Source Book*. Washington, DC: NASA Reference Publication 1024; 1978.
18. Weistroffer JK, Mills WJ, Shin AY. Recurrent rupture of the triceps tendon repaired with hamstring tendon autograft augmentation: a case report and repair technique. *J Shoulder Elbow Surg*. 2003;12(2):193-196.
19. Windisch G, Tesch NP, Grechenig W, Peicha G. The triceps brachii muscle and its insertion on the olecranon. *Med Sci Monit*. 2006;12(8):BR290-BR294.